| 1. Report No. FHWA/TX-06/5-3969-01-1 | 2. Government Accession No. | 3. Recipient's Catalog No. |
|---|---|---|
| 4. Title and Subtitle<br>Implementation of Laser Device for Highway Speed Macro-Texture Measurement | | 5. Report Date<br>October 2004<br>Published: July 2006 |
| | | 6. Performing Organization Code |
| 7. Author(s)<br>Richard Liu, Yuanhang Chen, Xuemin Chen, Jing Li and Wei Sun | | 8. Performing Organization Report No.<br>5-3969-01-1 |
| 9. Performing Organization Name and Address<br>Department of Electrical and Computer Engineering<br>University of Houston<br>4800 Calhoun Rd.<br>Houston, TX 77204-4005 | | 10. Work Unit No. |
| | | 11. Contract or Grant No.<br>5-3969-01 |
| 12. Sponsoring Agency Name and Address<br>Texas Department of Transportation<br>Research and Technology Implementation Office<br>P.O. Box 5080<br>Austin, TX 78763-5080 | | 13. Type of Report and Period Covered<br>Technical Report:<br>September 1, 2003 – August 31, 2004 |
| | | 14. Sponsoring Agency Code |

15. Supplementary Notes
Project performed in cooperation with the Texas Department of Transportation and the Federal Highway Administration.
Project title: Non-Contact Skid System
URL: http://tti.tamu.edu/documents/5-3969-01-1.pdf

16. Abstract:

In project 7-3969, the researchers had successfully developed a new, cheaper high speed texture laser for texture data collection. Based on the project 7-3969, 15 laser-based units which are capable of measuring pavement macro-texture at highway speed are delivered in this project.

Compared with the old laser device developed in Project 7-3969, the new version developed in this project has significantly reduced the size, weight, and noise levels, and has improved the standoff distance, measurement range and accuracy.

In this report, the laser triangulation method is briefly reviewed. Then, the improvement over the old laser device and the calibration procedures are also presented.

| 17. Key Words<br>Laser, Macro Texture, Laser Triangulation, Position Sensitive Device | | 18. Distribution Statement<br>No restrictions. This document is available to the public through National Technical Information Service, Springfield, Virginia, 22161, www.ntis.gov | |
|---|---|---|---|
| 19. Security Classif. (of this report)<br>Unclassified | 20. Security Classif. (of this page)<br>Unclassified | 21. No. of Pages<br>26 | 22. Price |

**Form DOT F 1700.7** (8-72) Reproduction of completed page authorized

This form was electrically by Elite Federal Forms Inc.

# Implementation of Laser Device for Highway Speed Macro-Texture Measurement

**by**

***Richard Liu, Yuanhang Chen, Xuemin Chen, Jing Li and Wei Sun***

**Technical Report 5-3969-01-1**

Project Number: 5-3969-01
Project title: Non-Contact Skid System

Performed in Cooperation with the
Texas Department of Transportation
and the
Federal Highway Administration

by the

Subsurface Sensing Laboratory
Department of Electrical and Computer Engineering
University of Houston

October 2004
Published: July 2006

# DISCLAIMERS

The contents of this report reflect the views of the authors, who are responsible for the facts and the accuracy of the data presented herein. The contents do not necessarily reflect the official view or policies of the Federal Highway Administration (FHWA) or the Texas Department of Transportation (TxDOT). This report does not constitute a standard, specification, or regulation.

University of Houston
4800 Calhoun Rd.
Houston, TX 77204

# ACKNOWLEDGMENTS

We greatly appreciate the financial support from the Texas Department of Transportation that made this project possible. The support of the Implementation Director, Brian Michalk, is also very much appreciated. We also thank the OPR/Construction Division director Thomas Bohuslav.

# Table of Contents

# List of Figures



# List of Tables

# CHAPTER 1: INTRODUCTION

## 1.1 PROJECT OVERVIEW

Highway skid number is largely dependent on the macro-texture of the pavement. For many years, TxDOT uses skid truck to measure skid number directly. The skid truck is a trailer with a standard weight. During the skid measurement, brake is applied to the trailer. This measurement is direct and accurate. However, measurement speed is limited and frequent traffic slow down is inevitable. For years, TxDOT has been pursuing alternative skid measurement methods using laser and other NDT tools such as laser and microwave. Two major components are included in order to achieve a non-contact skid measurement. The first component is to investigate short-range sensors that are sensitive to micro- and macro-texture. The second one is to relate the skid number to the measured data. In project 7-3969, the researchers had successfully developed a new, cheaper high speed texture laser for texture data collection. Based on the project 7-3969, 15 laser-based units which are capable of measuring pavement macro-texture at highway speed are delivered in this project.

Compared with the old laser device developed in Project 7-3969, the new version developed in this project has significantly reduced the size, weight, and noise levels, and has improved the standoff distance, measurement range and accuracy.

In this report, the laser triangulation method is briefly reviewed. Then, the improvement over the old laser device and the 15 units' calibration results are also presented.

# CHAPTER 2: SYSTEM DESIGN AND SPECIFICATIONS

## 2.1 PRINCIPLE OF LASER TRIANGULATION METHOD

The triangulation method is the most widely-used approach in modern industry, especially in surface inspection. Having the advantages of low cost, simplicity, robustness and good resolution, the laser-optic triangulation has been widely applied to both profiling and gauging applications [1]. It provides the capabilities of high speed, non-contact and high accuracy [2].

There are several parameters pertaining to a range sensor that indicate the system performance. These parameters include sampling rate, stand-off distance, measurement range and measurement resolution (accuracy). The laser-based triangulation system consists of a laser diode, an optical positioning system, a signal generation and processing circuitry and a data acquisition and analysis system.

Two components constitute the optical system of the triangulation-range-sensing device: the laser beam and image-generation mechanism and the position-sensitive-detector (PSD) system. In the following section the mathematical formulation of the triangulation method is presented [3].

The concept of optical triangulation is illustrated in Figure 1. In this technique, a collimated laser beam illuminates the measurement surface. The target surface reflects the beam, which is then focused on the position-sensitive-detector, and forms a beam spot. The beam spot moves on the PSD as the surface height changes. The displacement of the surface can then be determined by detecting the movement of the beam spot.

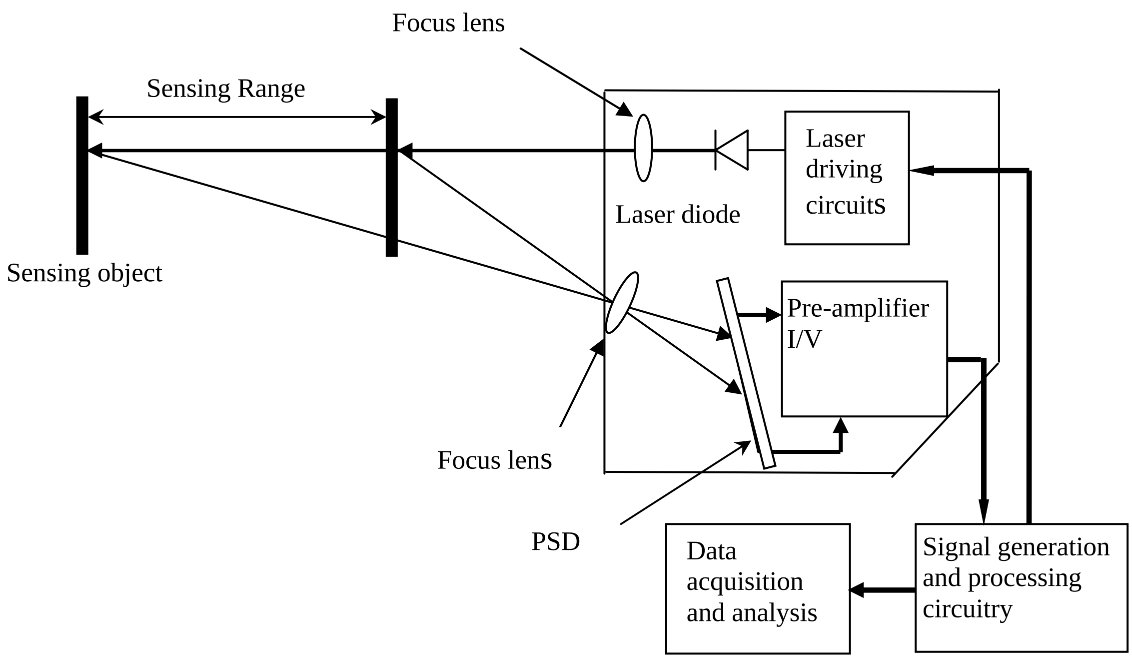


Figure 1 Laser-based triangulation system.

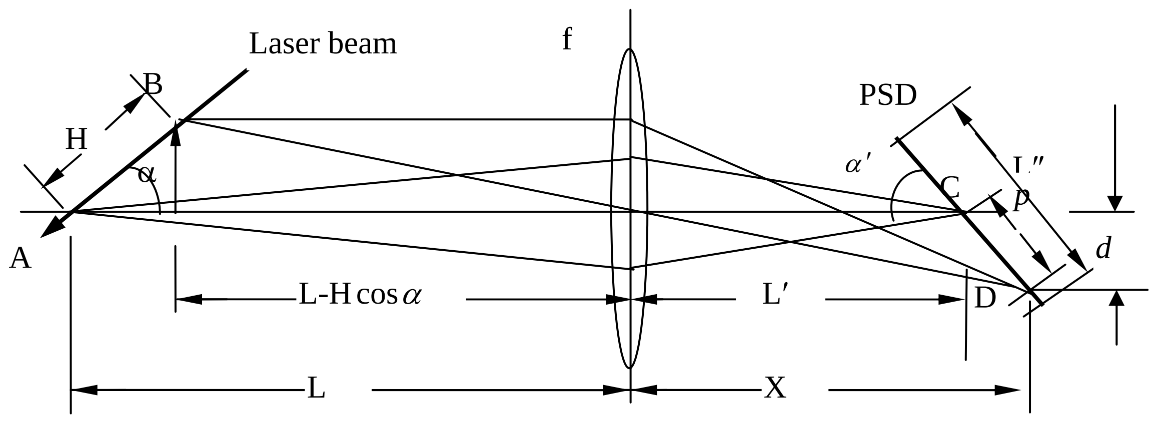


Figure 2 Triangulation principle.

Figure 2 illustrates the geometry of image formation. Assume that the laser beam intercepts the optical axis at point A, and the virtual image of A is located at point C (on the axis). Image B corresponds to point D. According to the law of image focusing, the following relationships can be established:

$$\frac{1}{f} = \frac{1}{L} + \frac{1}{L'} \ , \tag{1}$$

and

$$\frac{1}{f} = \frac{1}{L - H\cos\alpha} + \frac{1}{X} , \tag{2}$$

where H is the change of height (from point A to point B) and α is the formation angle (viewing angle) of the image. From Equations (1) and (2), L′ and X can be expressed by Equation (3) and Equation (4),

$$L' = \frac{Lf}{L - f} \ , \tag{3}$$

and

$$X = \frac{f(L - H\cos\alpha)}{L - H\cos\alpha - f} . \tag{4}$$

The heights of point B and its image D comply with the law of image magnification, which states

$$\frac{d}{H\sin\alpha} = \frac{X}{L - H\cos\alpha} , \tag{5}$$

where *d* is the height of the image. Substitute X using Equation (4), then *d* can be expressed as

$$d = \frac{fH\sin\alpha}{L - H\cos\alpha - f} . \tag{6}$$

To find out $\alpha'$, the angle of PSD with the main optical axis, we subtract Equation (3) from Equation (4) and get

$$X - L' = \frac{f(L - H\cos\alpha)}{L - H\cos\alpha - f} - \frac{fL}{L - f},$$

$$= \frac{f^2 H\cos\alpha}{(L - f)(L - H\cos\alpha - f)}. \tag{7}$$

Therefore, the slope of line segment CD is

$$\tan\alpha' = \frac{d}{X - L'} = \frac{fH\sin\alpha}{L - H\cos\alpha - f} \times \frac{(L - f)(L - H\cos\alpha - f)}{f^2 H\cos\alpha'},$$
$$= \frac{(L - f)}{f}\tan\alpha,$$
$$= const. \tag{8}$$

The displacement of $p$ can be read out directly from the circuitry output. From Equation (9),

$$\frac{1}{f} = \frac{1}{H\sin\alpha} + \frac{1}{p\sin\alpha'}, \tag{9}$$

$H$ can be calculated by Equation (10):

$$H = \frac{fp\sin\alpha'}{(p\sin\alpha' - f)\sin\alpha} \tag{10a}$$

or

$$p = \frac{Hf\sin\alpha}{(H\sin\alpha - f)\sin\alpha'}. \tag{10b}$$

In the macro/micro system design, two factors need to be taken into account: the choice of the imaging lens and the distance between the imaging lens and the object. The intensity of the reflected light is very weak (in μW). To increase the energy from the reflected light, a lens with a bigger size is adopted. Therefore, the spot focused on the PSD is strong enough so that the PSD can generate stable signals with low noise level. However, the mounting requirement limits the size of the lens. It is impossible to get a large lens in short focus without creating an image distortion. The distance from the lens to the object is a major parameter affecting the light energy collected by the imaging lens. The shorter the distance, the more energy from the spot enters the imaging lens. In design, a diameter of 50mm plano-convex lens (focus 50mm) is utilized as the imaging lens. The distance from the lens to the pavement is set to 50mm (stand off distance). Therefore, the parameters in the formulas given in Equation (1) through Equation (10) are $\alpha$ = 35°, $L$= 113mm (to the optical center of the lens), $\alpha'$ = 41.42° and $L'$= 89.683mm respectively.

Based on the Triangulation principle, the brief system structure is shown on Figure 3.

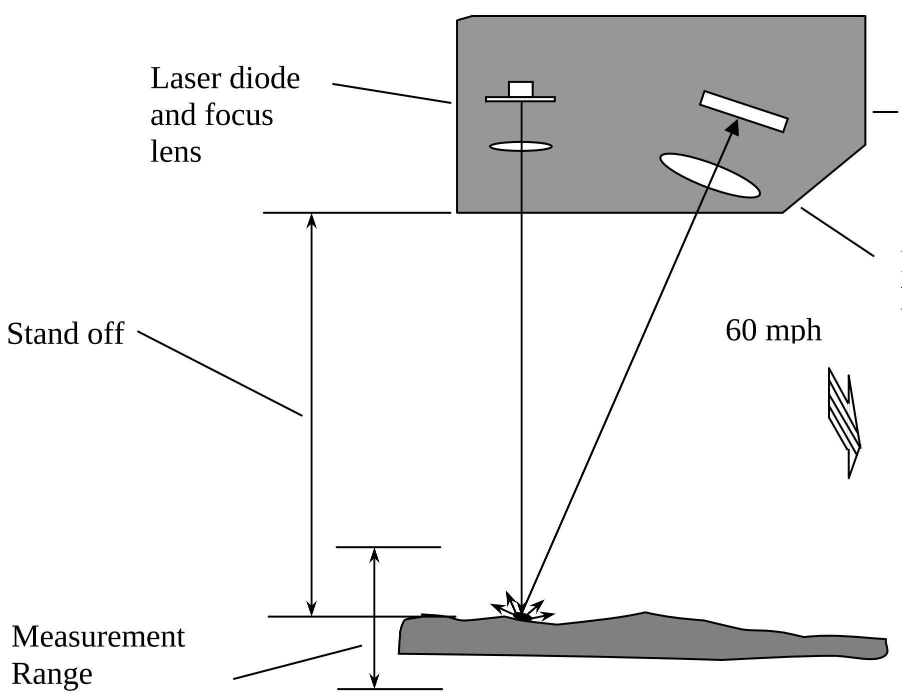


Figure 3 Measurement on pavement surface.

## 2.2 SYSTEM STRUCTURE AND IMPROVEMENTS

The developed laser unit is shown in Figure 4.

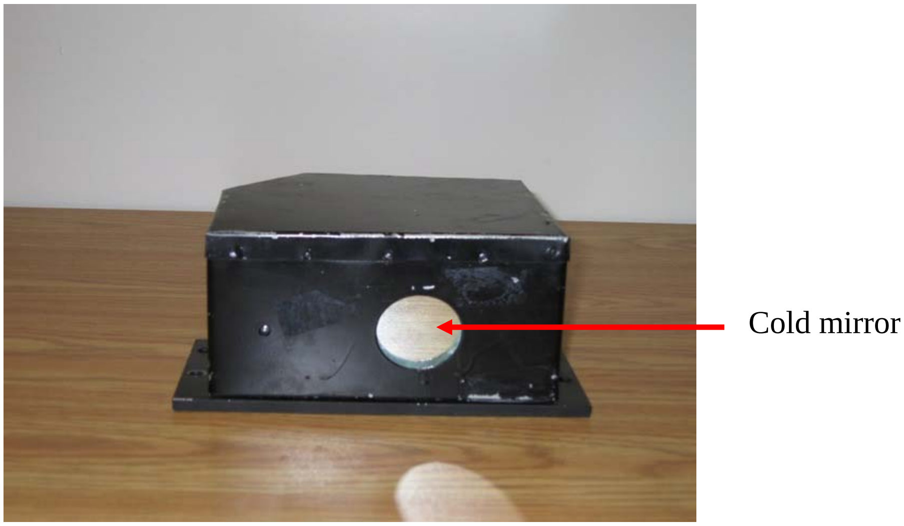


Figure 4 The laser device based on triangulation method.

The internal structure of the laser device is shown in Figure 5.

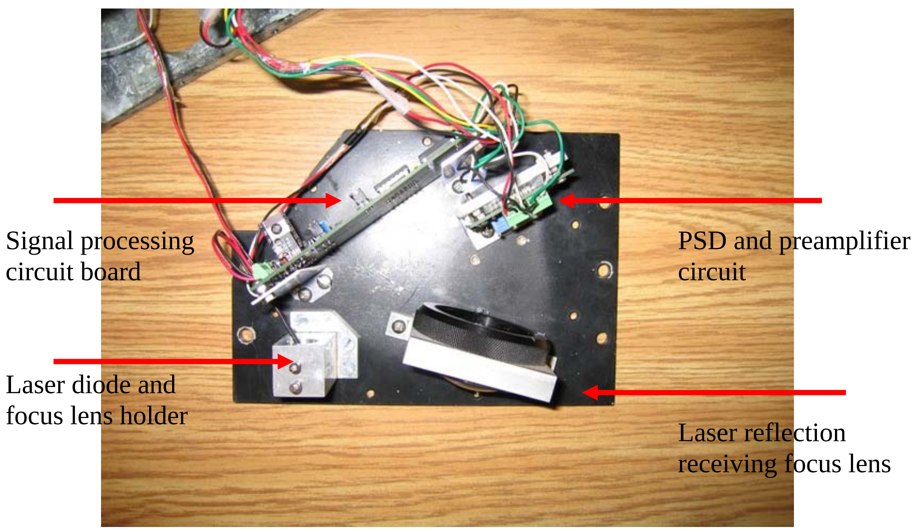


Figure 5 The inner hardware configuration.

Compared with the laser device developed in Project 7-3969, several improvements have been made to reduce the system noise and gain the system performance.

### 2.2.1 Reduce the unit size and increase the standoff distance

With carefully recalculating the optical configuration, the laser box size has reduced 30% compared with the old version. The standoff distance has increased to 12” from the 6” of the previous version without losing accuracy.

### 2.2.2 Separate the PSD signal condition circuit

To reduce the noise level, the PSD signal condition circuit was separated from the signal processing circuit. The PSD preamplifier circuit is shown in Figure 6.

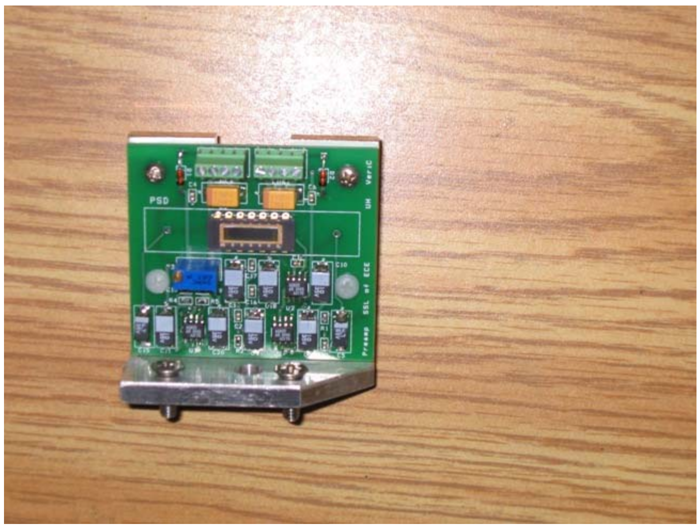

Figure 6 PSD preamplifier circuit.

### 2.2.3 Cold mirror

Cold mirror has a dielectric coating that is designed to reflect the visible region of the spectrum and transmit the infrared. A cold mirror was applied before the laser refection receiving focus lens.

## 2.3 SPECIFICATIONS OF THE TEXTURE LASER

The specifications of the pushcart-mounted device are described as follows:

1. Standoff distance: 12 inches

The standoff distance means the distance between the laser source and object.

2. Data update rate: 150 KHz

The laser source is operated at the frequency range of 150 KHz.

3. Maximum range of measured thickness: $\pm 3$ inches

This detector has been verified to detect a thickness change of 6 inches.

4. System clock: 1.5 MHz

5. Size: 8.44 inches (L) x 6.02 inches (W) x 3.65 inches (H)

6. Average power consumption: 0.8 A at 12 V

# CHAPTER 3: LASER DEVICES CALIBRATION

## 3.1 LASER DEVICE CALIBRATION PROCEDURES

1. Set up the distance between laser and measuring object as 30.48 cm.

2. Turn on the power supply for the laser device.

3. Record the voltage output of laser sensor at 30.48 cm standoff distance.

4. Moving the measured object forward and backward 7.62 cm separately, record the voltage output change every 0.5 cm.

5. Use Excel or Matlab to plot the voltage output versus 15.24 cm distance change.

6. Get the second order curve fit equation from the measured points.

7. Use the second order curve fit equation to convert the measured voltage into distance.

According to the calibration procedures, the calibration data for the laser set 1 is shown Table 1.

Table 1 Voltage versus Distance of Set # 1

(The Standoff Distance between edge of laser box and surface is 280mm.)

| Set #1 / **Distance** | VOLTS (V) | DIFF (V) 2.5 mm | DIFF (V) 5 mm |
|---|---|---|---|
| 255mm | 3.853 | 0.484 | 0.96 |
| 257.5mm | 3.369 | 0.476 | |
| 260mm | 2.893 | 0.446 | 0.849 |
| 262.5mm | 2.447 | 0.403 | |
| 265mm | 2.044 | 0.356 | 0.672 |
| 267.5mm | 1.688 | 0.316 | |
| 270mm | 1.372 | 0.324 | 0.6409 |
| 272.5mm | 1.048 | 0.3169 | |
| 275mm | 0.7311 | 0.3116 | 0.6023 |
| 277.5mm | 0.4195 | 0.2907 | |
| **280mm** | 0.1288 | | |
| 282.5mm | -0.1435 | 0.2723 | 0.541 |
| 285mm | -0.4122 | 0.2687 | |
| 287.5mm | -0.6698 | 0.2576 | 0.5129 |
| 290mm | -0.9251 | 0.2553 | |
| 292.5mm | -1.183 | 0.2579 | 0.5129 |
| 295mm | -1.438 | 0.255 | |
| 297.5mm | -1.703 | 0.265 | 0.546 |
| 300mm | -1.984 | 0.281 | |
| 302.5mm | -2.253 | 0.269 | 0.551 |
| 305mm | -2.535 | 0.282 | |

### 3.2 REFERENCE FOR CONVERTING VOLTAGE INTO DISTANCE

If measured distance is in the range between -10mm and 10mm of standoff distance (280mm), Figure 7 is the voltage versus distance curve.

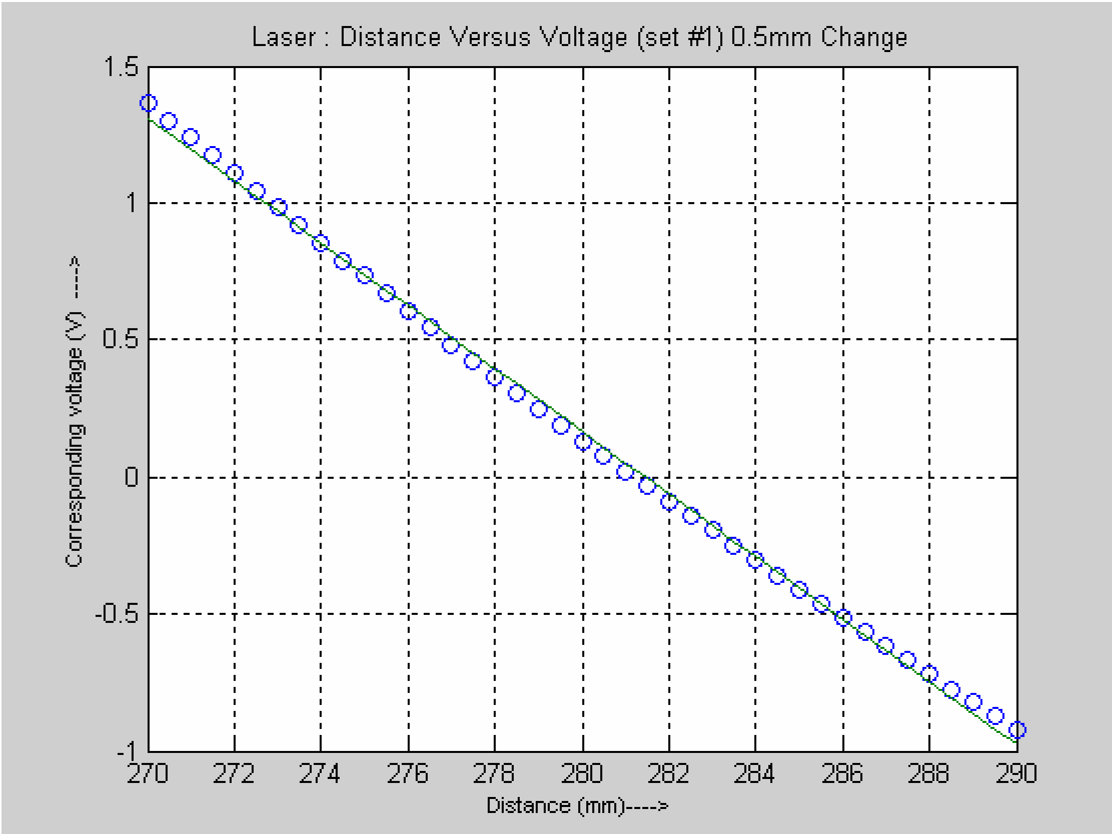


Figure 7 Distance vs. Voltage of laser set 1.

By using polynomial fit, we can find the relationship between voltage and distance:

$$V = -0.1143 \times D + 32.1773 \quad (11)$$

where V is measured Voltage and D is corresponding distance.

By using Equation (11), the distance information can be converted by the following equation:

$$D = (32.1773 - V) \div 0.1143 \quad (12)$$

If measured distance is in the range between -25mm and 25mm of standoff distance (280mm), Figure 8 is voltage versus distance curve.

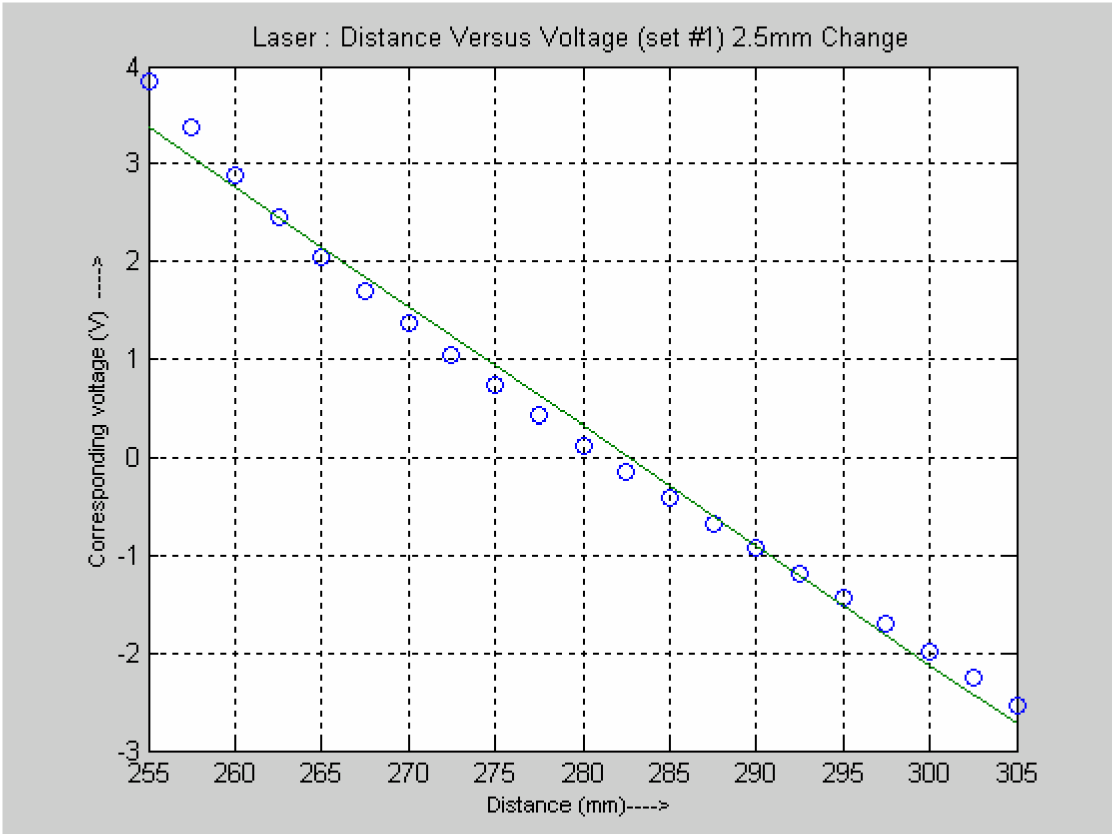


Figure 8 Distance vs. Voltage (laser set 1) measurement with 2.5mm change.

By using polynomial fit, we can find the relationship between voltage and distance:

$$V = -0.1221 \times D + 34.5005 \tag{13}$$

where V is measured Voltage and D is corresponding distance.

By using Equation (13), the distance information can be converted by the following equation:

$$D = (34.5005 - V) \div 0.1221 \tag{14}$$

# CHAPTER 4: RECOMMENDATIONS

In this project, we successfully implemented the 15 units of macro-texture laser device. But it still has some room to improve. The first one is the cold mirror. The cold mirror significantly reduces the ambient light effects. But the PSD output still can reach saturation when the laser device working under the strong sunshine. A laser line filter may resolve this problem. The other issue with the device is durability. We used the metal sheet to make the cover box. It may be not strong enough for the daily data collection. The mechanical improvement should be done in the future design.

## REFERENCES


1. G. Bazin, and B. Journet, “A New Laser Range-Finder Based on FMCW-like Method,” *IEEE Instrumentation and Measurement Technology Conference*, pp. 90-93, 1996.

2. C. F. M. Manuel, “Surface Inspection by an Optical Triangulation Method,” *Opt. Eng.*, **35**(9), pp. 2743-2747, 1996.

3. David R. Wiese, “Laser Triangulation Sensors: A Good Choice for High Speed Inspection,” *Chilton’s I&CS (Instrumentation and Control System)*, **62**, pp, 27-29, 1989.